

Noise and vibration reduction with vibroacoustic metamaterials on a cover for power electronics of an electric powertrain

Sebastian Rieß, Marvin Droste, A. Erraji, J. Córdor López, Karsten Finger, Heiko Atzrodt

<http://dx.doi.org/10.25673/103514>

Abstract

Vibroacoustic metamaterials are a promising technology for broadband noise and vibration reduction, that can induce a stop band for vibrations in the frequency domain. Within the stop band no elastic wave propagation is possible. Individually designed for the target structure, vibroacoustic metamaterials can be integrated neutrally in terms of weight and package. Therefore, they are especially suited for the use in the automotive industry where light weight structures are employed, which are more prone to vibrations. In the presented work the integration of a vibroacoustic metamaterial into a cover of power electronics of an electric powertrain is investigated. Therefore, a cover with integrated vibroacoustic metamaterial is numerically designed and experimentally tested in terms of acoustics and structural dynamics. The vibroacoustic metamaterial is integrated by cutting an array of resonators into the cover. For damping and sealing of the cover, the slots are filled in one configuration with silicone. In another configuration the cover is equipped with a PVC foil. For performance evaluation the developed covers with vibroacoustic metamaterial are benchmarked against an add-on vibroacoustic metamaterial approach commonly used in literature as well as against state-of-the-art measures for noise and vibration reduction like alubutyl and bitumen-layers, larger wall thicknesses and sandwiched steel sheets with an integrated damping layer. The developed covers for the power electronics of an electric car with integrated vibroacoustic metamaterial feature amplitude reductions of more than 30 dB for structural vibrations and more than 10 dB for the radiated sound power within the stop band region compared to the reference cover.

Kurzfassung

Vibroakustische Metamaterialien sind eine vielversprechende Technologie zur breitbandigen Reduktion von Vibrationen und Lärm. Sie sind in der Lage Stoppbänder im Frequenzbereich auszubilden. Innerhalb solcher Stoppbänder ist keine elastische Wellenausbreitung möglich. Genau abgestimmt auf die Zielstruktur,

lassen sich vibroakustische Metamaterialien gewichts- und bauraumneutral in Bauteile integrieren und eignen sich daher im Besonderen für den Einsatz in der Automobilindustrie, wo schwingungsanfällige Leichtbaustrukturen eingesetzt werden. In der vorliegenden Arbeit wird die Integration vibroakustischer Metamaterialien an einem Deckel der Leistungselektronik eines elektrischen Antriebsstrangs untersucht. Dazu wird ein Deckel mit integriertem vibroakustischen Metamaterial numerisch ausgelegt und experimentell hinsichtlich Akustik und Strukturmechanik bewertet. Das vibroakustische Metamaterial wird durch das Hineinschneiden eines Arrays verteilter Resonatoren in den Deckel integriert. Um Dämpfung hinzuzufügen und um den Deckel abzudichten, werden in einer Deckel-Konfiguration die bestehenden Schlitzlöcher mit Silikon gefüllt. In einer weiteren Konfiguration wird der Deckel mit einer PVC-Folie beklebt. Für die Bewertung der Performance hinsichtlich Schwingungs- und Schallreduktion werden die entwickelten Deckel mit vibroakustischem Metamaterial mit einem in der Literatur üblichen add-on vibroakustischen Metamaterials sowie mit Maßnahmen nach dem aktuellen Stand der Technik zur Geräusch- und Schwingungsreduktion wie Alubutyl- und Bitumenschichten, einer Wandstärkenvergrößerung und Sandwich-Blechen mit integrierter Dämpfungsschicht verglichen. Die entwickelten Deckel für die Leistungselektronik eines Elektrofahrzeugs mit integriertem vibroakustischen Metamaterial weisen im Vergleich zum Referenzdeckel Amplitudenreduktionen für Strukturschwingungen von mehr als 30 dB und für die abgestrahlte Schallleistung von mehr als 10 dB im Stoppbandbereich auf.

1. Introduction

The decarbonization of the automotive industry shifts the development of individual mobility towards battery electrified vehicles to fulfill the determined consumption targets. Consequently, automotive manufacturers integrate light weight structures into the electric vehicle to enlarge the driving range and to reduce the CO₂ emissions of their fleet. From the functional perspective like Noise Vibration Harshness (NVH) the insertion of light weight concepts, which are more prone to vibration, leads to additional challenges during development. At the same time, NVH requirements of electric vehicles are becoming increasingly important due to the missing acoustic masking effects emitted by internal combustion engines. Furthermore, one of the most important quality criteria perceived by the customer is indicated by the overall interior noise level. The main emitting noise source is identified by the electric drive unit, which is composed of the electric motor, the transmission, and the power electronics [1] (see Figure 1). The latter is shielded by a thin-walled steel cover, which is striking in terms of its acoustics due to its flat geometrical shape. The corresponding emerging frequency range is commonly between 400 to 1500 Hz. To increase NVH performance heavy weighted countermeasures like damping layers are applied to reduce the radiated noise of the cover. In this context, vibroacoustic metamaterials (VAMM) are a promising light weight technology for noise and

vibration reduction. Moreover, VAMM can play a major role during NVH development.

In the scope of the presented work, multiple cover configurations with an integrated VAMM are designed and benchmarked in terms of structural dynamic behavior and acoustic emission to conventional measures. Additionally, an add-on VAMM as commonly known from literature is designed and benchmarked against the cover with integrated VAMM. Conventional measures under investigation are the enlargement of the cover's thickness, a bitumen and alubutyl layer and the manufacturing of the cover from a sandwich sheet metal called bondal®.

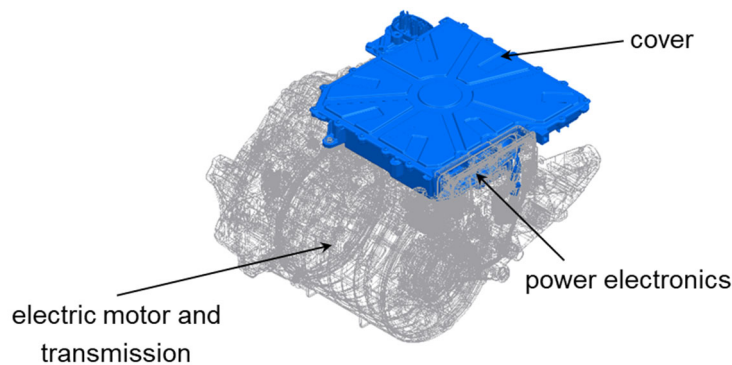


Figure 1: Electric drive unit with power electronics of an electric vehicle.

2. Vibroacoustic Metamaterials

Vibroacoustic metamaterials with local resonators are a novel technology for noise and vibration reduction, which are particularly promising for the use with light weight structures, such as they are used in the automotive industry. VAMMs induce a stop band for elastic waves in the frequency domain, where almost no wave propagation is possible. They consist of an array of distributed mechanical resonators, which are all tuned to the same resonance frequency (see Figure 2 (a)). They are placed at a distance smaller than half the wavelength of the vibration that is targeted. The resonator itself consists of a mass, spring, and damping element. The mechanical resonator and a part of the target structure form a unit cell. Applying the Bloch's Theorem [2], the stop band behavior of an infinite, periodic VAMM can be predicted by calculating the dispersion curve of a single unit cell. Figure 2 (b) shows an example of a dispersion curve, where the gap indicates the stop band. The starting frequency of the stop band is given by the resonance frequency of the resonator. The width depends on the oscillating mass and damping. A schematic representation of the stop band in the frequency domain is shown in Figure 2 (c). Further information about the fundamentals of VAMM can be found in [3]. For an overview on different VAMM designs and configurations the reader is referred to [4].

The application of VAMM to automotive parts has been investigated in various works. VAMM have been evaluated for the use in vehicle doors [5–7], the firewall [8], the roof [9] and the rear wheel arche [10]. VAMM are often produced using 3D-printing,

but also large-scale production processes have been investigated like punching and bending [5–7] or thermoforming [11]. The use of VAMM for noise and vibration reduction on covers for power electronics in electric vehicles has been investigated by the authors in [4] in a preliminary study.

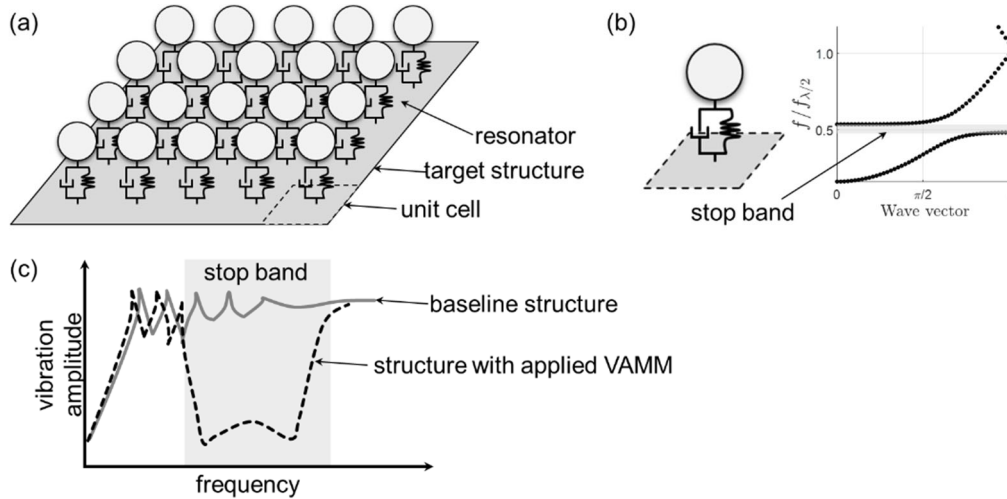


Figure 2: (a) VAMM consisting of an array of distributed resonators, (b) predicted stop band in the dispersion curve and (c) stop band in the frequency-domain.

3. Numerical design of the VAMM

For the comparison of standard measures for noise and vibration reduction on the forementioned cover, two different VAMM approaches have been numerically designed and built. To save weight and fulfill package requirements, an integrated VAMM approach has been developed, where no additional mass is added. This approach is tested in combination with different damping mechanisms. In another approach, a so-called add-on VAMM has been developed, where the resonators are made from elastomer pillars with an additional mass. This approach was chosen since it is common in academic studies. For all VAMM configurations, the frequency range between 400 to 1500 Hz is targeted. The wavelength at 400 Hz of the 2 mm thick steel cover is approx. 224 mm, so the size of the unit cells should be below 112 mm.

3.1 Integrated VAMM

For the integrated VAMM approach a concept already tested for a circular saw blade in [12] was used. The resonators are cut into the cover forming flaps, which are free to oscillate. The developed unit cell, in its first eigenmode is shown in Figure 3 (a). To predict the stop band behavior of the periodic VAMM compound the dispersion curve is investigated for 2D wave propagation. Applying the Bloch's Theorem, the wave propagation in the periodic VAMM compound can be predicted by a single unit cell.

For an undamped system, a stop band can be identified as a frequency region where no free wave propagation is possible. As can be seen in Figure 3 (b) a stop band is obtained in the frequency range of 400 to 600 Hz. The cover with the integrated 44 resonators is shown in Figure 3 (c).

To widen the stop band, damping may be added. The effect of different damping mechanisms, namely the integration of a viscoelastic material (silicone) into the slots as well as the attachment of a polymeric film onto the cover have not been evaluated numerically, but within experiments, as described in the following sections. Despite the damping effect, these measures are necessary to seal the cover.

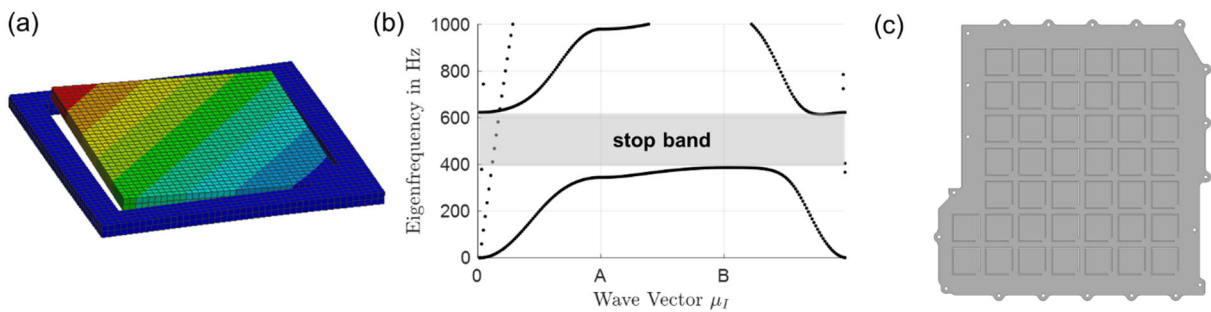


Figure 3: (a) Unit cell of the integrated VAMM in its first eigenmode. (b) Dispersion curve of the unit cell with predicted stop band. (c) Cover with integrated resonators.

3.2 Add-on VAMM

Since in literature most VAMM are built as add-on VAMM with attached resonators to the host structure an add-on VAMM configuration for comparison was elaborated for the cover as well. For that elastomer cylinders with an attached cylindrical mass element have been designed. The unit cell of size 50 mm x 50 mm in its first eigenmode can be seen in Figure 4 (a). The mass element weights 8.1 g adding a weight of approx. 24% (together with the weight of the elastomer pillars) of the host structure. For the elastomer a polyurethane rubber with a shore hardness of A50 was chosen.

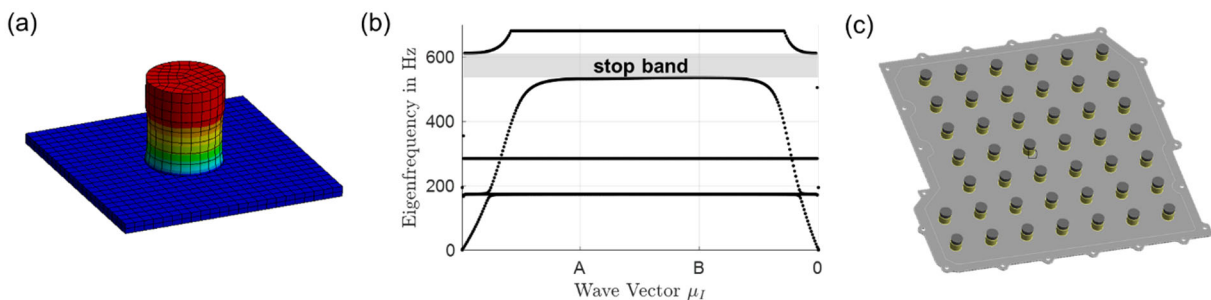


Figure 4: (a) Unit cell of the add-on VAMM in its first eigenmode. (b) Dispersion curve of the unit cell with predicted stop band. (c) Cover with applied resonators.

Figure 4 (b) shows the dispersion curve of the unit cell with a stop band in the frequency range from approx. 530 to 610 Hz. Due to the large, expected damping of the polyurethane rubber, which is not accounted for in the unit cell modelling, the expected stop band range is likely to start well before that and expand beyond the upper calculated stop band frequency. The effect is investigated experimentally in the following sections.

4. Cover demonstrators

In total nine cover configurations have been investigated. They are summarized in Table 1 together with their mass in relation to the reference cover without any measure.

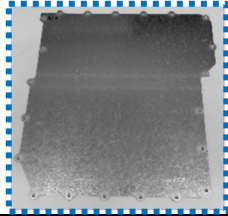
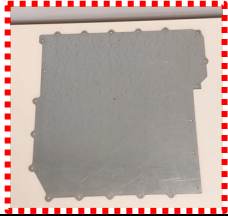
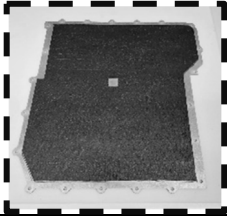
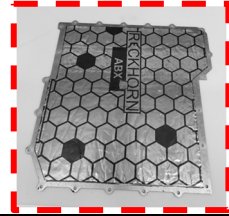
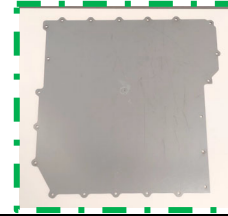
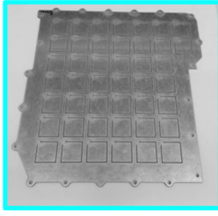
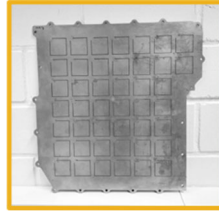

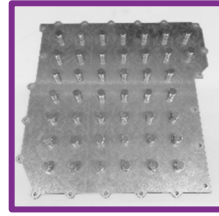
The reference cover with a thickness of 2 mm is the first cover which serves as a reference (1). Another reference cover with a thickness of 3 mm was chosen to investigate the influence of the increase in mass by 50% (2).

To compare the results of the VAMM covers with state-of-the-art measures for vibration reduction, one cover was equipped with a 2.5 mm thick bitumen layer (3) and another one with a 2 mm thick alubutyl layer (4). The bitumen adds 27% and the alubutyl 19% mass in relation to the 2 mm reference cover. Another state-of-the-art measure is the use of sandwich steel sheet metal with an integrated damping layer. So, another cover (5) was built from bondal® CB40, which consist of two 1 mm steel layers and a 0.04 mm damping layer.

As numerically designed in section 3.1, covers with integrated VAMM have been built. To incorporate the slots, a water jet cutting machine was used. In total three covers have been manufactured this way. The first cover remained without any additional damping measure (6), while the slots of the second one were filled with silicon (7) and the third one was equipped with a PVC foil (8) with a thickness of 0.11 mm (3M Wrap Film 2080). All those configurations weigh about 2-3% less than the 2 mm reference cover.

In the last configuration 44 elastomer pillars were added to a cover forming an add-on VAMM as numerically designed in section 3.2. The resonators are attached using a double-sided adhesive tape commonly used in the automotive industry. The mass elements are manufactured using a water jet cutting machine and have been attached to the elastomer pillars with the same double sided adhesive tape. The weight is increased by approx. 24% in relation to the 2 mm reference cover.

Table 1: Cover configurations under investigation.

1) reference cover (2 mm)	2) reference cover (3 mm)	3) bitumen	4) alubutyl	5) bondal® CB40
				
baseline	+50% mass	+27% mass	+19% mass	-2% mass
6) integrated VAMM	7) integrated VAMM + silicone	8) integrated VAMM + PVC foil	9) add-on VAMM	
				
-3% mass	-3% mass	-3% mass	+24% mass	

5. Experimental investigation of the structural dynamic behavior

Structural dynamic measurements in terms of acceleration have been carried out on the cover configurations as described in section 4. The experimental setup is shown in Figure 5. The covers are suspended with elastic bands to ensure a free velocity boundary condition. The excitation is done using an electrodynamic shaker which is connected to the center of the cover with a piezoelectric force sensor. The sensor is used to measure the introduced dynamic force to calculate the acceleration. A bandlimited random noise (< 2000 Hz) signal was chosen for excitation. The surface velocities resulting from the excitation are measured with a laser doppler vibrometer in 20 points, as indicated in Figure 5 (red).

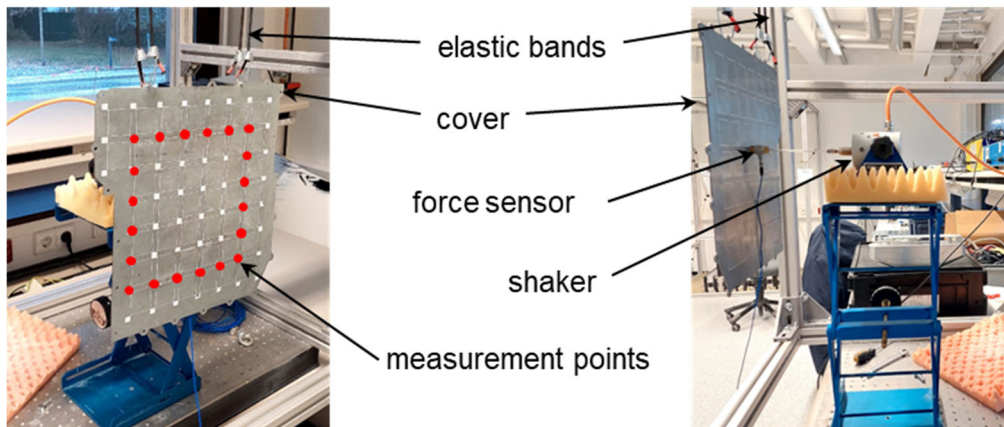


Figure 5: *Experimental setup of the structural dynamic measurements.*

The obtained measurement results as transfer function (TFF) in terms of accelerance, averaged over the 20 measurement points, are depicted in Figure 6 (a) for the VAMM configurations and (b) for the standard measures. In both scopes the TFFs are compared to the ones of the reference cover of thickness of 2 mm. Increasing the thickness of the cover to 3 mm leads to a reduction in amplitudes due to the increase in mass. Especially in the higher frequency range (above 1500 Hz) an amplitude reduction of up to 20 dB can be obtained. Before that, the amplitudes are comparable to the reference cover. Adding alubutyl or bitumen to the cover leads to a broadband amplitude reduction of about 30 dB. Due to the larger added mass of the bitumen layer the amplitudes above approx. 1000 Hz are reduced to a larger extend compared to the alubutyl configuration. The cover made from bondal® sheet metal performs comparably to the cover that is equipped with bitumen but is lighter by approx. 23 %. The large damping effect of bondal® likely is due to the placement of the damping material right in the neutral axis of the cover. Here, the shear deformation is largest taking full advantage of the damping capabilities of the damping layer.

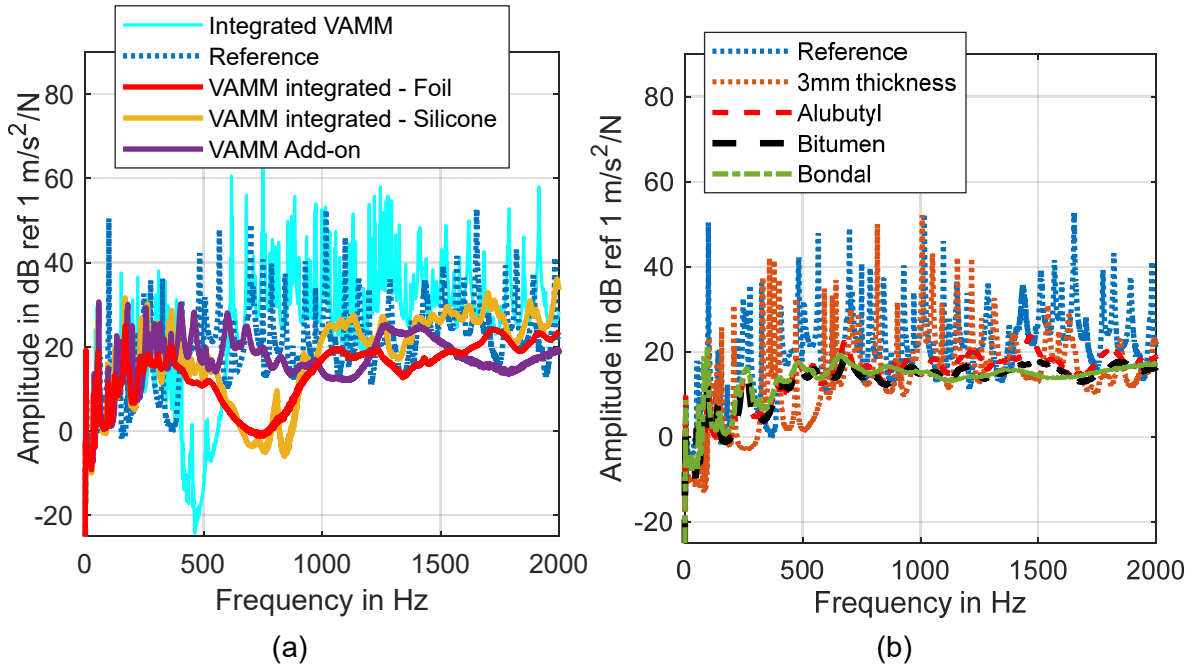


Figure 6: Transfer functions in terms of acceleration. (a) Reference cover and VAMM variants. (b) Reference cover, cover with thickness $d = 3$ mm and covers with damping materials.

Looking at the VAMM configurations in Figure 6 (a), larger amplitude reductions than with the standard measures can be achieved within the stop band frequency range. The cover with integrated VAMM without any damping measure behaves accordingly to the numeric simulations. The stop band starts at approx. 400 Hz and reaches until 600 Hz. The amplitude reduction within this range compared to the reference cover is larger than 60 dB. Before and after the stop band, larger amplitudes occur compared to the reference cover. This is due to the weakening of the cover by inserting the slots. By adding a damping medium this disadvantage can be compensated, as can be seen for the cover configurations with integrated VAMM and added damping in terms of silicone and the PVC foil. The stop band shifts to larger frequencies (approx. 450 – 1000 Hz) due to the stiffening effect of the foil and the silicone, but especially after the stop band the amplitudes are largely reduced. Especially the configuration with PVC film performs comparable to the reference covers with standard damping approaches. But compared to the covers with alubutyl and bitumen it is 18% and 23% lighter and features an amplitude reduction of approx. 15 dB in the stop band region. Compared to the cover made from bondal® sheet metal, the weight is almost the same, but within the stop band region an amplitude reduction by about 15 dB is achieved with the VAMM approach.

The add-on VAMM made from an array of elastomer pillars is characterized by large damping due to the material chosen. The stop band starts at approx. 600 Hz as predicted by the numeric simulations but extends over a larger frequency range as predicted (until 1250 Hz). This is due to the damping, which was neglected in the simulations.

6. Experimental investigation of the acoustical behavior

To investigate the acoustic behavior of the cover, the radiated noise is determined by performing an intensity probe test according to DIN EN ISO 9614-2 [13]. The scanning method from [13] is chosen and a cuboidal measurement area is selected, as shown in Figure 7. The covers are under free-free conditions and are excited by an electrodynamic shaker. The electrodynamic shaker is mounted at the center of the cover and the applied dynamic acceleration and dynamic force are measured with a piezoelectric mechanical impedance sensor. Encapsulation of the electrodynamic shaker reduces extraneous noise so that only the power radiated from the cover is measured. The experiments are performed in a semi-anechoic chamber (class 1).

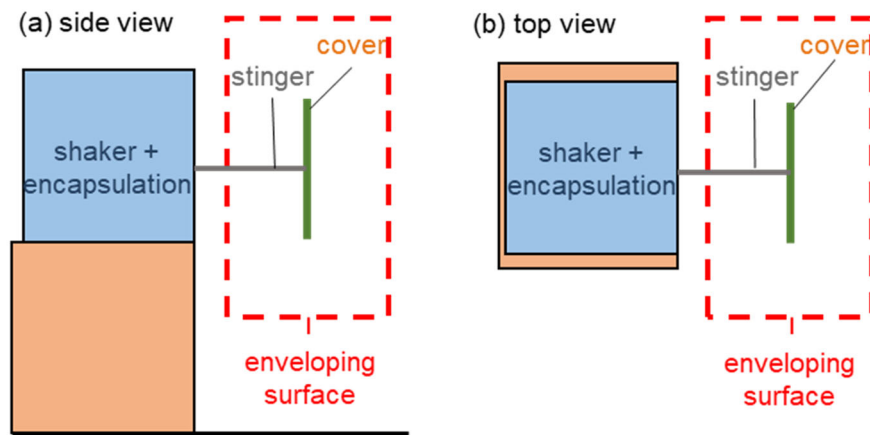


Figure 7: Sketch of measurement setup. (a) Side view and (b) top view of sound intensity measurements.

Figure 8 depicts the actual measurement setup for the covers. A cuboidal measurement area of $A = 5.53 \text{ m}^2$ is chosen. A white noise excites the covers with a frequency range of $100 \text{ Hz} \leq f \leq 2 \text{ kHz}$. The root mean squared accelerations of the white noise at the excitation point amount to $a_{\text{in}} = 2 \text{ m/s}^2$. To ensure valid calculated sound intensities for the whole frequency range, a sound intensity probe containing two microphones with a constant distance of $d = 12 \text{ mm}$ is used.

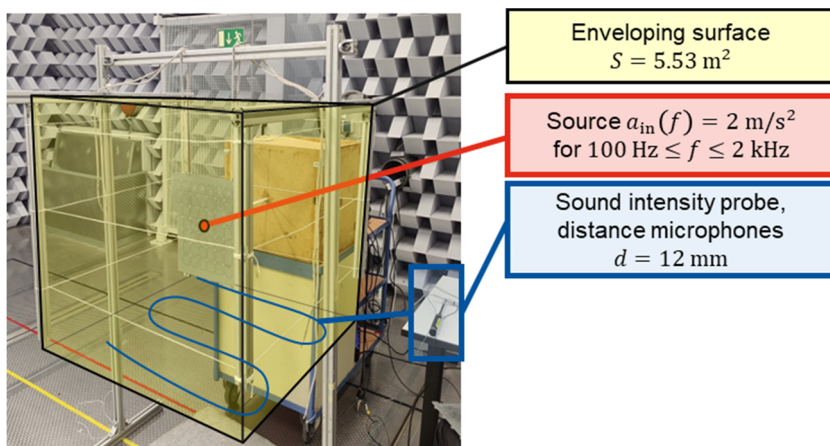


Figure 8: Measurement setup of the cover for sound intensity measurements.

The excitation force is different for each cover variant. To account for this in the description of the radiated sound power, the frequency spectrum of the excitation power P_{in} is calculated by multiplying the excitation force F_{in} and the particle velocity v_{in} at the excitation point [14] as shown in Equation (1).

$$P_{input} = \frac{1}{2} \cdot Re(F_{in} \cdot v_{in}^*) \quad (1)$$

The resulting spectra of the excitation powers for each cover variant are shown in Figure 9. The cover configuration with integrated VAMM without a damping measure was omitted from the study, since the structural dynamic measurements have shown, that the amplitudes before and after the stop band are much higher than the reference.

The excitation power of the VAMM variants decreases in the frequency range above the stop band region as shown in Figure 9 (a). The excitation power of the reference cover and the cover with thickness $d = 3$ mm varies greatly due to resonances and antiresonances. In addition, uncertainties in the peak positions may lead to discrepancies in the calculation of the ratio between excitation and radiated power due to not perfectly aligned peaks. For these reasons, third octave band values are chosen for the evaluation of the radiated efficiencies for each cover.

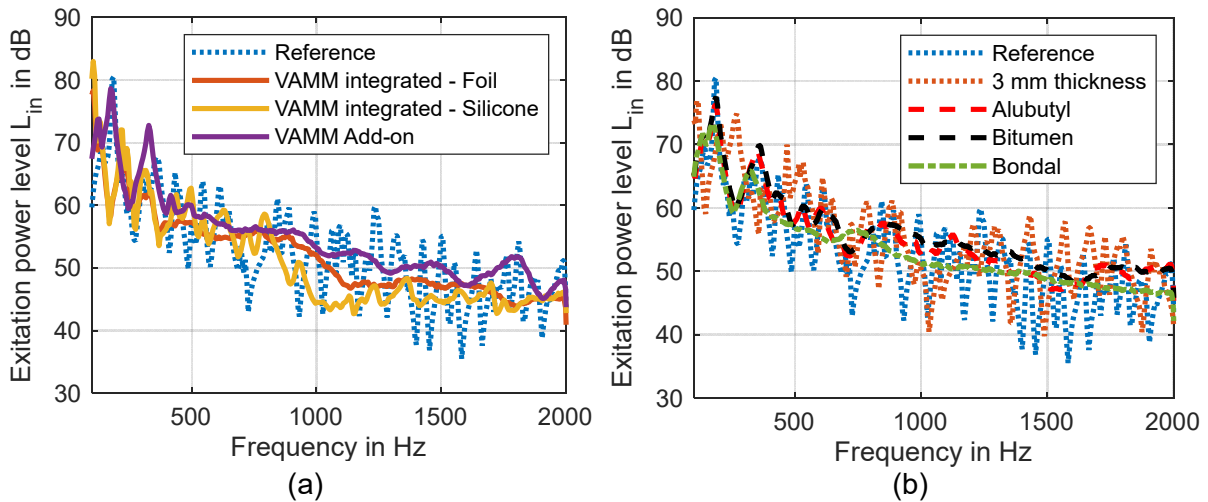


Figure 9: Spectra of excitation power levels at the excitation point of the covers with constant root mean squared dynamic acceleration at the excitation point. (a) Reference cover and VAMM variants. (b) Reference cover, cover with thickness $d = 3$ mm and covers with damping materials.

The VAMM variants have similar influences on the radiated sound power level (SWL) of the cover as shown in Figure 10. When excited with spectrally constant acceleration, the SWL of the VAMM variants is reduced in the frequency ranges of the stop bands as well as in the frequency range above the stop bands. Above the stop band, the radiated sound power of the integrated VAMM variants is further reduced, similar to the reduction of the excitation powers for these variants (Figure 10 (a)). The damping materials lead to a reduction of the radiated sound power in the

whole frequency range of $100 \text{ Hz} \leq f \leq 2 \text{ kHz}$.

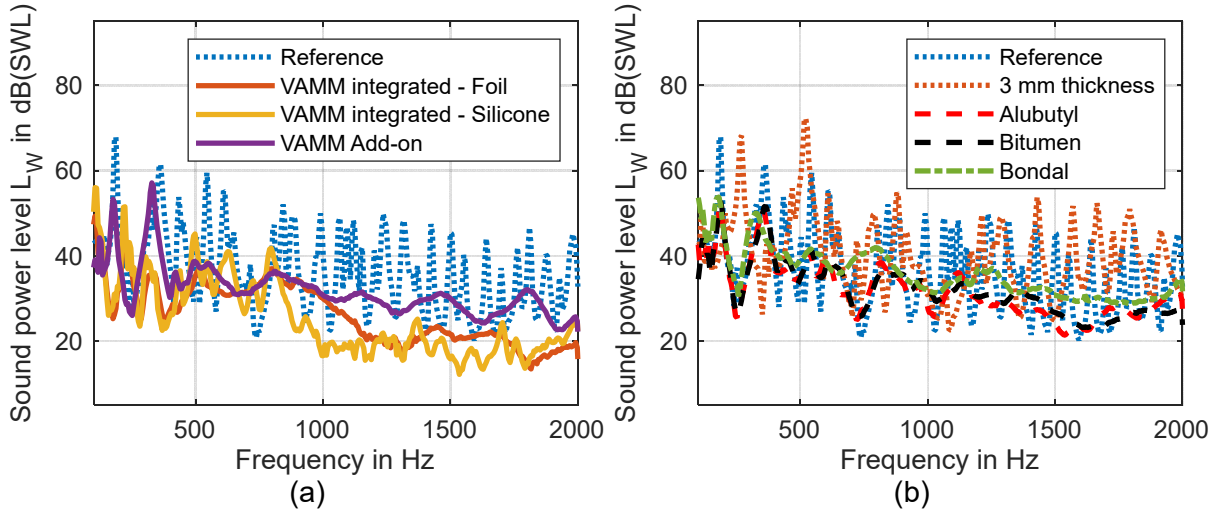


Figure 10: Spectra of radiated sound power levels of the covers with constant root mean squared dynamic acceleration at the excitation point. (a) Reference cover and VAMM variants. (b) Reference cover, cover with thickness $d = 3 \text{ mm}$ and covers with damping materials.

To compare the spectral reduction in radiated power of VAMM variants independent on the excitation power, the radiated sound power of the cover variant $P_{W,\text{variant}}$ is divided by the power at the excitation point of the cover variant P_{in} . The resulting radiation efficiency of the corresponding variant is compared with the radiation efficiency of the reference cover. Subsequently, the resulting difference of the radiation efficiencies ΔL_W is determined according to Equation (2).

$$\Delta L_W = 10 \log_{10} \frac{P_{W,\text{variant}}}{P_{\text{in},\text{variant}}} - 10 \log_{10} \frac{P_{W,\text{reference}}}{P_{\text{in},\text{reference}}} \quad (2)$$

Figure 11 depicts frequency dependent reductions of the radiation efficiency of the different cover variants. The radiation efficiency is reduced by $\Delta L_W \approx -10 \text{ dB}$ on average in the frequency ranges of the respective stop bands. The largest reduction of $\Delta L_W \approx -17 \text{ dB}$ is achieved in the third octave band with $f_{\text{mid}} = 400 \text{ Hz}$. Below the stop band, the average difference is $\Delta L_W \approx 0 \text{ dB}$, with variations for each third octave band most likely due to frequency shifts. Above the stop band, the radiated sound power levels of the VAMM configurations are slightly lower than the ones of the reference cover, which is most likely due to the added damping. Compared to that, the covers with damping materials as well as the cover with the additional thickness have a reduction of $\Delta L_W \approx 6 \text{ dB}$ in most frequency ranges.

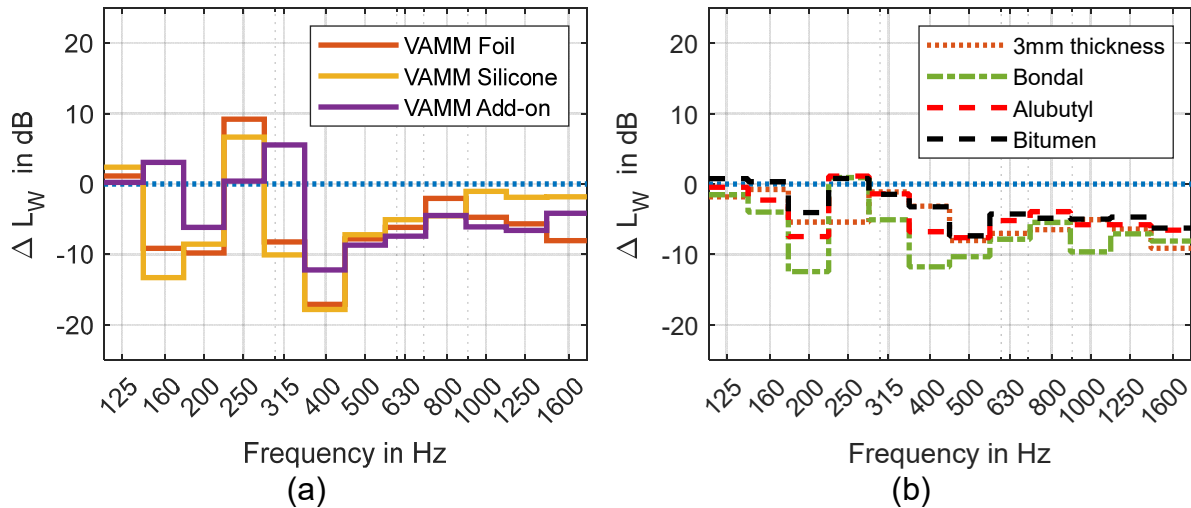


Figure 11: One-third octave spectra of difference between radiated sound power levels of the cover variants and the reference cover. (a) VAMM variants (b) Cover with thickness $d = 3$ mm and covers with damping materials.

7. Conclusion and outlook

In the presented work nine different configurations of a cover for power electronics of an electric drive unit have been built and tested. In total five different VAMM variants have been compared to a reference cover and to four different state-of-the-art measures for noise and vibration reduction, namely the enlargement of the wall-thickness, the addition of a bitumen and an alubutyl-layer as well as the use of sandwich sheet metal with an integrated damping layer (bondal®). VAMM configurations in terms of integrated VAMM in combination with different damping techniques and an add-on VAMM have been numerically designed and built.

All configurations have been tested in terms of the structural dynamic behavior and the radiated sound power. The integrated VAMM variants with additional damping (slots filled with silicone, attached PVC foil) feature a large amplitude reduction of about 15 dB in the stop band region in terms of acceleration compared to the standard measures (bitumen, alubutyl, bondal®). Above the stop band region, they perform comparably well as the standard measures. Below the stop band region amplitudes are higher than the standard measures. The same can be said for the radiated sound power. Within the stop band an amplitude reduction of approx. 10 dB compared to the standard measures bitumen and alubutyl and a reduction of 6 dB in comparison to the bondal® cover can be reached. Above the stop band the behavior is comparable.

In conclusion, the integrated VAMM covers with additional damping perform comparable to the standard measures like bitumen and alubutyl while being approx. 23% and 18% lighter and featuring a large amplitude reduction within the stop band of approx. 15 dB for vibrations and 10 dB for radiated sound power. While being as light as the bondal® cover, the integrated VAMM variants feature the advantage of a

large amplitude reduction within the stop band region.

As indicated by the measurement results integrated VAMMs are especially well suited to reduce components weight compared to bitumen and alubutyl or enhance the performance compared to bondal® sheet metal. Particularly they are beneficial to cut out bandlimited excitations with their stop band functionality, overcoming the performance of all the standard measures.

Further works will focus on integrating multiple stop bands into the cover with an integrated VAMM configuration and the investigation of covers within a vehicle.

8. References

- [1] Lieske, D., Landes, D., and Fischer, J.: Optimization of the Powertrain Noise for the Electric Vehicle Mercedes-Benz EQC. *ATZ Worldwide*, vol. 122, no. 3, pp. 56–61, 2020.
- [2] Bloch, F.: Über die Quantenmechanik der Elektronen in Kristallgittern. *Zeitschrift für Physik*, vol. 52, pp. 555–600, 1929.
- [3] Claeys, C.: Design and Analysis of Resonant Metamaterials for Acoustic Insulation. Dissertation KU Leuven, 2014.
- [4] Rieß, S., Droste, M., Atzrodt, H., Appel, N., Córdor López, J., Finger, K., Erraji, A., Troge, J.: Vibroacoustic metamaterials for noise and vibration reduction in the automotive industry: Aachen Acoustics Colloquium 2022, Aachen, Germany, 2022.
- [5] Riess, S., Droste, M., Manushyna, D., Melzer, S., Druwe, T., Georgi, T., Atzrodt, H.: Vibroacoustic Metamaterials for enhanced acoustic Behavior of Vehicle Doors: 15th International Congress on Artificial Materials for Novel Wave Phenomena – Metamaterials, pp. X-374–X-376, 2021.
- [6] Droste, M., Manushyna, D., Rieß, S., Atzrodt, H., Druwe, T., Melzer, S., Troge, J., Struß, A., Lühring, A., Clausen, J.: Application of vibroacoustic metamaterials in a vehicle door: DAGA 2022 - 48. Jahrestagung für Akustik, pp. 233–235, 2022.
- [7] Droste, M., Manushyna, D., Rieß, S., Atzrodt, H., Druwe, T., Melzer, S., Struß, A., Lühring, A.: Design and validation of production-suited vibroacoustic metamaterials for application in a vehicle door: DAGA 2021 - 47. Jahrestagung für Akustik, pp. 132–135, 2021.
- [8] Chang, K.-J., Jung, J., Kim, H.-G., Choi, D. R., Wang, S.: An Application of Acoustic Metamaterial for Reducing Noise Transfer through Car Body Panels. SAE Technical Paper 2018-01-1566, 2018.
- [9] Wan, Q., Shao, R.: A hybrid phononic crystal for roof application. *The Journal of the Acoustical Society of America*, vol. 142, no. 5, pp. 2988–2995, 2017.
- [10] Sangiuliano, L., Reff, B., Palandri, J., Wolf-Monheim, F., Pluymers, B., Deckers, E., Desmet, W., Claeys, C.: Low frequency tyre noise mitigation in a vehicle using metal 3D printed resonant metamaterials. *Mechanical Systems and Signal Processing*, vol. 179, 2022.
- [11] Melo Filho, N. de, Claeys, C., Deckers, E., Desmet, W.: Realisation of a thermoformed vibro-acoustic metamaterial for increased STL in acoustic resonance driven environments. *Applied Acoustics*, vol. 156, pp. 78–82, 2019.

- [12] Riess, S., Droste, M., and Atzrodt, H.: Noise Reduction of circular Saw Blades using Vibroacoustic Metamaterial: Sixteenth International Congress on Artificial Materials for Novel Wave Phenomena – Metamaterials, pp. X-362–X-364, 2022.
- [13] DIN EN ISO 9614-2:1996-12. Akustik - Bestimmung der Schalleistungspegel von Geräuschquellen aus Schallintensitätsmessungen - Teil 2: Messung mit kontinuierlicher Abtastung (ISO 9614-2:1996).
- [14] Karger, M.: Fluid-Struktur-Wechselwirkung in der Energie-Finite-Elemente-Methode. Dissertation, Technische Universität Hamburg-Harburg, 2017.